Available online at www.sciencedirect.com
SCIENCE DIRECT®
Journal of Sound and Vibration 268 (2003) 291–304
JOURNAL OF SOUND AND VIBRATION
www.elsevier.com/locate/jsvi

A stochastic approach to cable dynamics with moving rivulets

D.Q. Cao, R.W. Tucker*, C. Wang

Department of Physics, Lancaster University, Lancaster LA1 4YB, UK

Received 28 May 2002; accepted 11 November 2002

Abstract

This article constructs a stochastic model for the response of stay cables of cable-stayed bridges to the combined effect of wind and rain. It describes a spring-mounted section model of a stay cable in a steady wind where aerodynamic forces are modified by the dynamics of a mobile liquid rivulet. The motion of the rivulet is described by a simple stochastic process that, together with aerodynamic forces, models the complex fluid–structure interaction. Based on measured data for drag and lift coefficients and a static rivulet location, an analysis of the model suggests a new stochastic excitation mechanism for the rain–wind induced vibrations of stay cables.

1. Introduction

Long steel cables, such as are used in cable-stayed bridges and other structures, are prone to vibration induced by weather conditions and the structure to which they are connected. Such vibrations depend on the variation of many parameters that can influence the behaviour of a bridge structure. If the vibrations of the support (girders and/or towers) fall into certain frequency ranges, the movements of attached stay cables may become significant due to such parametric variation. In large-span cable-stayed bridges, parametric resonance of stay cables can be significant due to the presence of many low-frequency modes in the bridge deck and stay cables that may be excited. On the other hand, light-to-moderate wind combined with light-to-moderate rain alone has been observed to excite surprisingly large amplitude vibrations in stay cables in a number of cable-stayed bridges worldwide [1–3].

Extensive studies on the parametric excitation of stay cables have been published in the literature (see, for example, Refs. [4–6] and the references cited therein). For vibrations induced by weather conditions, rain–wind induced vibrations in stay cables have recently become of some

*Corresponding author. Tel.: +44-1524-593610; fax: +44-1524-844037.
E-mail address: r.tucker@lancaster.ac.uk (R.W. Tucker).

0022-460X/03/$ - see front matter
doi:10.1016/S0022-460X(03)00205-0

concern to bridge engineers in many countries (see, for example, Refs. [7–10] and the references cited therein). This paper seeks an insight into the mechanism leading to such vibrations from a simple stochastic model that attempts to capture their essential features.

It is believed that the underlying mechanism is similar to that producing "galloping" in cables that offer an asymmetric profile to aerodynamic flows, i.e., low-frequency, high-amplitude oscillations that can occur on a prismatic body such as an ice-coated electrical transmission line or an inclined stay cable in steady-side wind. For an ice-coated conductor, Den Hartog [11] introduced a stability criterion that specified conditions for galloping to occur. Since then, there have been extensive investigations of this phenomenon, including static and dynamic wind tunnel tests on a variety of cross-sections to determine their propensity to gallop. Recent research has focused on the study of coupled vertical and torsional galloping [12,13], coupled vertical and horizontal galloping [14,15], and coupled vertical, horizontal and torsional galloping [16–18]. The stability criteria given in the above literature are derived using the methods of deterministic aerodynamics and apply directly to prismatic bodies of fixed shape.

However, it has been pointed out that the existence of a *mobile* rain rivulet may also modify the aerodynamic forces on a stay cable and lead to a modified excitation mechanism. In wind tunnel tests, it was observed that the accretion of rain can effectively change the shape of a body by forming two thin agglomerations of liquid on its surface, whose position depends on wind pressure distribution, body motion and gravity forces [9]. From wind tunnel investigations Hikami and Shiraishi [1] argue that the origin of certain rain-induced cable vibrations is rivulet formation on the cable surface. Furthermore, the results of wind tunnel tests, using an experimental model of a cable with an artificial rivulet *fixed* on its surface, cannot be directly extrapolated to realistic cable vibration processes [10]. Such a model does not allow the rivulet(s) to react to wind action, cable motion and their mass inertia. Rivulet motion is expected to play an important role in determining the interaction between cable and rivulet and the changing pressure distribution around the cross-section of the cable.

The detailed motion of a cable under rain and wind forces is complex. To fully understand its behaviour even in light wind and rain involves the analysis of the equations of multi-phase fluid dynamics, a model for accretion and fluid–solid adhesion and the continuum mechanics of an elastic structure. Insight can however be gained by analyzing the incompressible fluid flow around an immersed rigid disc. In regimes where boundary layer separation occurs, nascent vortices can react on the disc and induce oscillatory motion. The separation points on its circumference often occur in pairs on opposite sides of a diameter and their motion can "lock" to that of the oscillating disc. It is believed that, for an appropriate Reynolds number, the location of these separation points might (in the presence of light rain) act as seeds for the concentration of an accretion layer of rain on the circumference. Without further detailed experimental information (or expensive time-consuming computational fluid dynamic simulations) it is difficult to assess how the buildup of rivulets on cylinders at such locations modify the subsequent aerodynamic flow around them particularly when the cylinder moves relative to the inflow fluid field. However, in low ambient wind speeds, experiments with an artificial mobile rivulet on a fixed cylinder subject to aerodynamic loading do indicate an approach to a steady rivulet oscillation. Describing the dynamic adhesive forces that bind the rivulets to the perimeter of the disc clearly constitutes a difficult modelling challenge. Once the profile of the rivulet is decided and its initial location on the disc ascertained one is confronted with the problem of estimating the aerodynamic forces and

couples on an asymmetric structure. Wind tunnel test on fixed discs for various rivulet configurations and wind speeds (in the plane of the disc) offer data for static configurations. They provide lift, drag and torque coefficients relative to the ambient wind tunnel velocity. In order to estimate these coefficients for a moving disc with a mobile rivulet relative to its circumference, the simple strategy of mapping these coefficients into the co-moving frame of the moving disc is adopted. To model the motion of a rivulet (which indirectly is determined by the complex dynamics of the boundary layers between the disc, rain and air), a simple stochastic equation is adopted which accommodates the observed steady state rivulet motion relative to the disc observed in static tests. This strategy is analogous to the use of "wake oscillator" models that have been used successfully to model vortex-induced vibrations on cylinders without recourse to computational fluid dynamics [19]. In further support for this strategy, it has been found that the deterministic component of such an equation arises naturally from an analysis of the dynamics of a small mobile mass free to move on a moving cylinder under the action of viscous Stokes's friction, non-inertial forces induced by the motion of the circumference in space and aerodynamic forces [20].

Under gravity, a stay cable sags into a catenary between two fixed supports. It is simpler to analyze a spring-supported damped section model shown in Fig. 1(a) rather than directly approach the full three-dimensional cable problem. Motivated by the above, this spring-mounted section model of a stay cable with one-degree-of-freedom motion in a steady wind with velocity perpendicular to its length was considered. The aerodynamic forces on it are modulated by a variable effective cross-section determined by the cable and the moving rivulet(s).

Although rivulets along both upper and lower cable surfaces have been observed in rain–wind conditions, it is generally believed that the upper one is the dominant one in inducing cable vibration. Thus, a single rivulet moving on the upper surface of a cable, under the influence of the wind, gravitational and friction forces will be considered. It will be modelled by a small added-mass undergoing stochastic motion on the circumference. The motion will be described by the

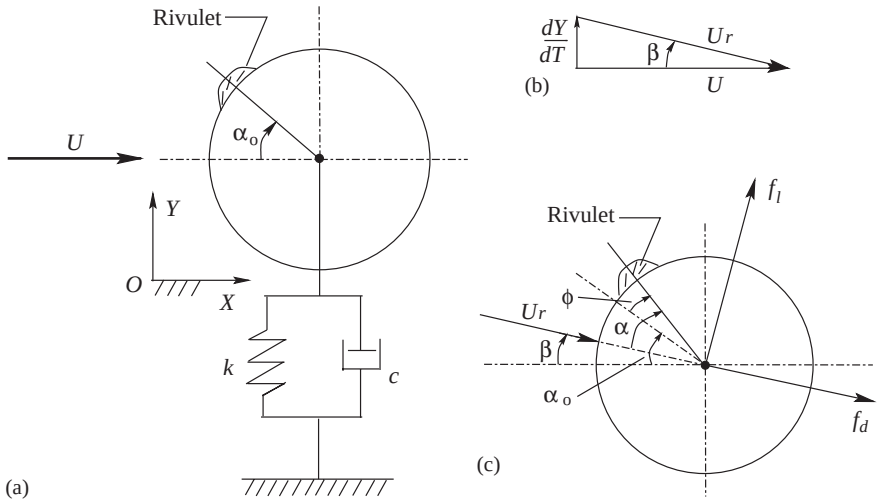

Fig. 1. (a) Location of rivulet on the surface of the cable; (b) dynamic angle of relative velocity; (c) schematic diagram of the aerodynamic forces.

response of a band-pass filter. Such a filter can be thought of as an ideal system that, when excited by white noise input, gives a response whose power spectral density (PSD) induces the PSD of the moving rivulet. Using this filter and the reported experimental values of steady wind force coefficients for a cable section model with an artificial static rivulet [7], and data for its location [1], a stochastic dynamic model will be developed and solved in order to investigate the onset of rain–wind-induced vibrations of stay cables.

2. Stochastic model of a cable section with a rivulet

The spring-supported model exposed to a steady wind of velocity U blowing from left to right has an asymmetric cross-section, a spring stiffness k, a structural damping coefficient c, and a mass m per unit length (including the rivulet under wind–rain conditions). The wind will always generate a drag force on the cable, and, in wind–rain conditions, a randomly moving rivulet of water on the surface of the cable can cause a positive or negative lift force on it. Typically, both the lift and drag vary with the location of the rivulet on the surface of the cable. When the rivulet moves irregularly, the lift and drag will vary randomly and can be described as stochastic processes. A quasi-steady analysis of the lift and drag can be determined from steady-state measurements, where an artificial rivulet is fixed on the surface of cable, i.e., the relative cable-attitude to wind is characterized by a given angle $\alpha = \alpha_0$ as shown in Fig. 1(a).

If the section model translates vertically with speed $\mathrm{d}Y/\mathrm{d}T$ at time T, then the relative speed of the wind, as shown in Fig. 1(b), can be derived from

$$U_r^2 = U^2 + \left(\frac{\mathrm{d}Y}{\mathrm{d}T}\right)^2, \quad \tan\beta = \frac{1}{U}\frac{\mathrm{d}Y}{\mathrm{d}T}. \tag{1}$$

The angle of the wind relative to the rivulet (the angle of attack α) is defined in the aerodynamic sense. The angle α measured clockwise from the relative wind to the location of the rivulet as shown in Fig. 1(c) is

$$\alpha = \alpha_0 + \phi - \beta, \tag{2}$$

where α_0 is the static angle of the rivulet and $\phi = \phi(T)$ is the fluctuation angle that describes the motion of the rivulet on the cable perimeter.

The lift and drag forces on the model per unit length (as shown in Fig. 1(c)) are

$$f_l = \tfrac{1}{2}\rho_a D U_r^2 C_l, \quad f_d = \tfrac{1}{2}\rho_a D U_r^2 C_d, \tag{3}$$

where ρ_a is the fluid (air) density, D is the cable diameter, $C_l = C_l(\alpha)$ and $C_d = C_d(\alpha)$ are the dimensionless lift and drag coefficients, respectively, which should be measured in a wind tunnel test for a given Reynolds number. The net vertical aerodynamic force on the model per unit length is

$$f_y = f_l \cos\beta - f_d \sin\beta = \tfrac{1}{2}\rho_a D U_r^2 (C_l \cos\beta - C_d \sin\beta). \tag{4}$$

The equation for vertical motion is taken to be

$$m\frac{\mathrm{d}^2 Y}{\mathrm{d}T^2} + c\frac{\mathrm{d}Y}{\mathrm{d}T} + kY = f_y. \tag{5}$$

Let the structural damping factor $\xi_0 = c/2m\omega_n$, where $\omega_n = \sqrt{k/m}$ is the fundamental frequency of the undamped system. Introducing the dimensionless displacement $y = (\omega_n/U)Y$ and time $t = \omega_n T$, Eq. (5) can be written as

$$\ddot{y} + 2\xi_0\dot{y} + y = \frac{1}{mU\omega_n} f_y, \tag{6}$$

where the dot $\cdot$ denotes the differentiation with respect to t. With the dependence of C_l and C_d on the angle of attack α determined from measurements, the dynamic force f_y can be rewritten as

$$f_y(\phi, \beta) = \tfrac{1}{2}\rho_a D U^2 (1 + \tan^2\beta)(C_l(\alpha)\cos\beta - C_d(\alpha)\sin\beta), \tag{7}$$

where the angle of attack α is itself a function of ϕ and β defined by Eq. (2).

Expanding the dynamic force $f_y(\phi, \beta)$ as a Taylor series expansion with respect to the variable ϕ and β about $\phi = 0$ and $\beta = 0$, gives

$$f_y(\phi, \beta) = \tfrac{1}{2}\rho_a D U^2 [C_l(\alpha_0) + C_l'(\alpha_0)\phi - (C_l'(\alpha_0) + C_d(\alpha_0))\beta] + \cdots, \tag{8}$$

where the prime $'$ denotes the differentiation with respect to the angle α.

If the maximum speed of the cable is much less than the wind speed, that is,

$$\frac{1}{U}\frac{\mathrm{d}Y}{\mathrm{d}T} = \frac{1}{U}\frac{U}{\omega_n}\frac{\mathrm{d}y}{\mathrm{d}t}\omega_n = \dot{y} \ll 1 \tag{9}$$

it follows from Eq. (1) that $\beta \approx \dot{y}$. Thus, neglecting the high order terms in $f_y(\phi, \beta)$, Eq. (6) becomes

$$\ddot{y} + 2\xi_0\dot{y} + y = \frac{\rho_a D U}{2m\omega_n}(C_l(\alpha_0) + C_l'(\alpha_0)\phi(t) - (C_d(\alpha_0) + C_l'(\alpha_0))\dot{y}). \tag{10}$$

Let

$$b_0 = \frac{\rho_a D U}{2m\omega_n} C_l(\alpha_0), \quad b_1 = \frac{\rho_a D U}{2m\omega_n} C_l'(\alpha_0),$$
$$\xi = \xi_0 + \frac{\rho_a D U}{4m\omega_n}(C_l'(\alpha_0) + C_d(\alpha_0)). \tag{11}$$

Note that the term b_0 causes a constant displacement, essentially a shift in the co-ordinate, and does not affect the dynamic behaviour of the system. Taking $\bar{y} = y - b_0$, Eq. (10) can be rewritten as

$$\ddot{\bar{y}} + 2\xi\dot{\bar{y}} + \bar{y} = b_1\phi(t). \tag{12}$$

As discussed above the system becomes stochastic if one adopts a stochastic process for ϕ. In a wind tunnel investigation it has been reported [1] that, when a cable executes steady vibrations in a rain environment, a rivulet can oscillate on the surface of the cable with the same period as the cable lateral motion. Thus, the stochastic equation for the moving rivulet will be described by a narrowband stochastic process. This motivates the authors to introduce a narrowband filter equation with a Gaussian stochastic source to describe its motion. Such a filter is an idealization. When excited by a white-noise input it yields a non-white stationary PSD. Now write

$$\ddot{\phi} + 2\xi_f\omega_f\dot{\phi} + \omega_f^2\phi = \sqrt{S_0}\eta(t), \tag{13}$$

where the constants $\omega_f (\approx 1)$, ξ_f and S_0 will be chosen in such a way to minimize the difference between the PSD of $\phi(t)$ and the effective PSD of the moving rivulet measured from wind–rain

tunnel tests or field measurements. The white-noise source $\eta(t)$ has zero mean, i.e., the PSD of $\eta(t)$ and the corresponding correlation function are, respectively,

$$S_\eta(\omega) = 1, \qquad R_\eta(\tau) = 2\pi\delta(\tau), \tag{14}$$

where δ is the Dirac δ distribution.

3. Stochastic responses

It is clear that if the damping factor ξ is negative, Eq. (12) yields unstable solutions. This suggests that the cable with an upper rivulet could become unstable according to the Den Hartog mechanism, depending on the location of the rivulet. When $\xi \leqslant 0$, the large amplitude dynamic behaviour of the cable should be determined by higher terms of the expansion of the aerodynamic forces. Consequently, a non-linear stochastic model should be developed to properly analyze the non-linear behaviour of the cable.

In practical situations, however, the absolute value of $C_l'(\alpha)$ is expected to be rather small for rivulets of small size relative to the diameter of the cable. This leads to positive aerodynamic damping, and the Den Hartog mechanism is not directly useful as an explanation of wind–rain-induced vibration. In the case of positive aerodynamic damping, since the excitation process $\eta(t)$ is assumed stationary and Gaussian, the response process of the linear system will also be stationary (once transients have decayed away) and Gaussian. Therefore, both input and output processes are completely specified by their means and correlation functions, or PSD functions. It follows from Eqs. (12) and (13) that the complex frequency transfer functions are, respectively,

$$H_{\bar{y}}(\omega) = \frac{b_1}{(1 - \omega^2 + 2\mathrm{i}\xi\omega)}, \quad H_\phi(\omega) = \frac{\sqrt{S_0}}{(\omega_f^2 - \omega^2 + 2\mathrm{i}\xi_f\omega\omega_f)}. \tag{15}$$

The PSD of the fluctuation angle $\phi(t)$ can then be obtained as

$$S_\phi(\omega) = H_\phi(\omega)H_\phi^*(\omega)S_\eta(\omega) = \frac{S_0}{((\omega_f^2 - \omega^2)^2 + 4\xi_f^2\omega^2\omega_f^2)}, \tag{16}$$

where $*$ denotes complex conjugation. Moreover, the PSD of the response $\bar{y}(t)$ is

$$\begin{aligned} S_{\bar{y}}(\omega) &= H_{\bar{y}}(\omega)H_{\bar{y}}^*(\omega)S_\phi(\omega) = H_{\bar{y}}(\omega)H_{\bar{y}}^*(\omega)H_\phi(\omega)H_\phi^*(\omega)S_\eta(\omega) \\ &= \frac{S_0 b_1^2}{[(1 - \omega^2)^2 + 4\xi^2\omega^2][(\omega_f^2 - \omega^2)^2 + 4\xi_f^2\omega^2\omega_f^2]}. \end{aligned} \tag{17}$$

The correlation function $R_\phi(\tau)$ can be determined directly from

$$R_\phi(\tau) = \int_{-\infty}^{+\infty} S_\phi(\omega)\mathrm{e}^{\mathrm{i}\omega\tau}\,\mathrm{d}\omega = \int_{-\infty}^{+\infty} \frac{S_0\mathrm{e}^{\mathrm{i}\omega\tau}}{(\omega_f^2 - \omega^2)^2 + 4\xi_f^2\omega^2\omega_f^2}\,\mathrm{d}\omega. \tag{18}$$

Setting $\tau = 0$, the integral can now be evaluated by standard methods to obtain the square of the standard deviation of the fluctuation angle $\phi(t)$. Thus, from Eq. (18),

$$\sigma_\phi^2 = R_\phi(0) = \int_{-\infty}^{+\infty} \frac{S_0}{(\omega_f^2 - \omega^2)^2 + 4\xi_f^2\omega^2\omega_f^2}\,\mathrm{d}\omega = \frac{\pi S_0}{2\xi_f\omega_f^3}. \tag{19}$$

Similarly, from Eq. (17), the square of the standard deviation of the stochastic response $\bar{y}(t)$ is

$$\begin{aligned}\sigma_{\bar{y}}^2 &= R_{\bar{y}}(0)\\ &= \int_{-\infty}^{+\infty} \frac{S_0 b_1^2}{[(1-\omega^2)^2+4\xi^2\omega^2][(\omega_f^2-\omega^2)^2+4\xi_f^2\omega^2\omega_f^2]}\,\mathrm{d}\omega\\ &= \frac{\pi S_0 b_1^2}{2\omega_f^3}\,\frac{[(\xi+\xi_f\omega_f)(1+\omega_f^2+4\xi\xi_f\omega_f)-\omega_f(\xi_f+\xi\omega_f)]}{[(\xi+\xi_f\omega_f)(\xi_f+\xi\omega_f)(1+\omega_f^2+4\xi\xi_f\omega_f)-\omega_f((\xi+\xi_f\omega_f)^2+(\xi_f+\xi\omega_f)^2)]}.\end{aligned}$$

Hence, from Eq. (19)

$$\frac{\sigma_{\bar{y}}^2}{\sigma_\phi^2} = \frac{[\xi(1+4\xi_f^2\omega_f^2)+\xi_f\omega_f(\omega_f^2+4\xi^2)]b_1^2}{[\xi((1-\omega_f^2)^2+4\xi_f^2\omega_f^2)+4\xi^2\omega_f(\xi_f+\xi_f\omega_f^2+\xi\omega_f)]}. \tag{20}$$

The means of the response $\bar{y}(t)$ and the fluctuation angle $\phi(t)$ can be obtained directly by taking expectations of the terms in Eqs. (12) and (13) as

$$m_{\bar{y}} = 0, \qquad m_\phi = 0. \tag{21}$$

Thus, $m_y = m_{\bar{y}} + b_0 = b_0$ and $\sigma_y = \sigma_{\bar{y}}$.

The spectra of the velocity $\dot{\bar{y}}$ can be found by using the relation $S_{\dot{\bar{y}}}(\omega) = \omega^2 S_{\bar{y}}(\omega)$. The stochastic response derived above makes it possible to carry out parametric studies and to evaluate the responses amplitude of the stay cables in wind–rain environments.

4. Numerical results and discussion

The steady stochastic properties of the random variables y and ϕ follow from the solutions above. The stochastic averages involve material parameters that are taken to describe stay cables in air and aerodynamic data from wind tunnel tests. The diameter D and the mass m per unit length of the stay cable are chosen as 180 mm and 26 kg/m, respectively. The air density is taken as 1.293 kg/m^3. The natural frequency ω_n is assumed to be 2.12 rad/s.

The experimental values of steady wind force coefficients for an aluminium circular cylinder with an artificial rivulet in the shape of a *fixed* solid sphere with diameter d ($d/D = 0.1$) were reported in Ref. [7] as shown in Fig. 2. [1] The drag and lift coefficient curves are fitted first to express the coefficients as functions of the attack angle α and then to obtain their derivatives of different orders. As indicated in Ref. [7], the diameter ratio of 0.1 is considered to be larger than the actual diameter ratio of rivulet to cable.

According to a wind tunnel test with rain conditions as reported in Ref. [1], the static angle α_0 of the rivulet[2] is a function of the mean wind speed U, as shown in Fig. 3.

Employing the relation between the static angle α_0 of the rivulet and mean wind speed, the damping factor ξ is actually a function of mean wind speed U. Based on Eq. (11), the variations of ξ with mean wind speed U for a set of structural damping ratios ξ_0 are depicted in Fig. 4. It can be observed that, within a certain range of wind speed, the damping factor ξ is negative in the case of

[1] The reference position of the angle of attack is different from that in Ref. [7].

[2] The reference position of α_0 is different from that in Ref. [1].

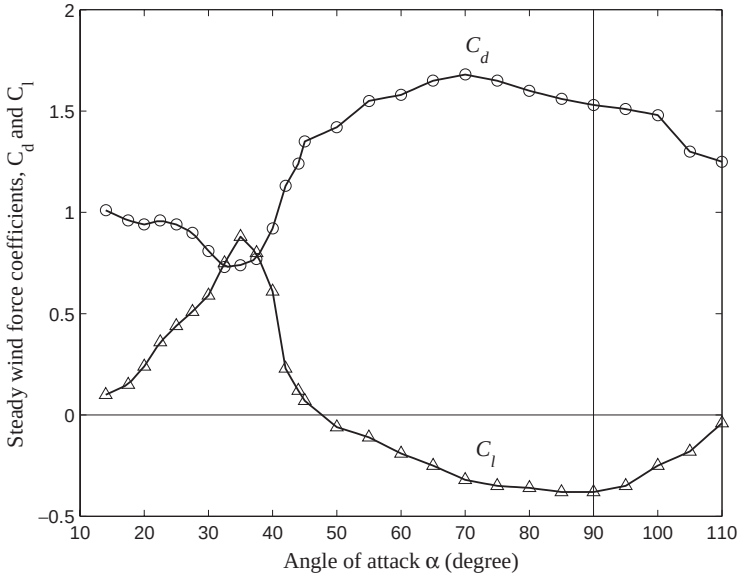

Fig. 2. Coefficients of drag and lift for a wind tunnel model with artificial rivulet.

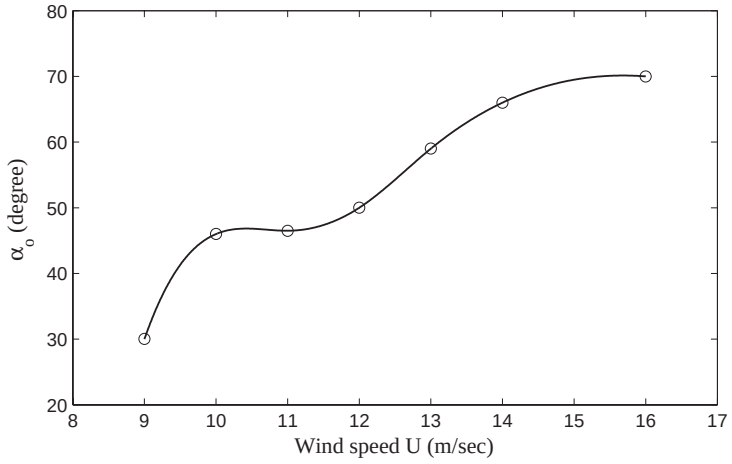

Fig. 3. Rivulet position versus wind speed.

a small structural damping ratio ξ_0. If ξ is negative, the cable is unstable and galloping occurs. The onset wind speed of galloping relates to the structural damping ratio ξ_0.

Similarly, b_0 and b_1 are functions of mean wind speed because of the relation between the static angle α_0 of the rivulet and mean wind speed. Based on Eq. (11), the amplitude of b_1 with mean wind speed is depicted in Fig. 5. It is interesting to note that, at about 9.2 m/s wind speed, the amplitude of b_1 increases rapidly with increasing wind speed until the peak amplitude is reached. After the peak amplitude, the amplitude of b_1 decreases to a lower level with further increase of wind speed.

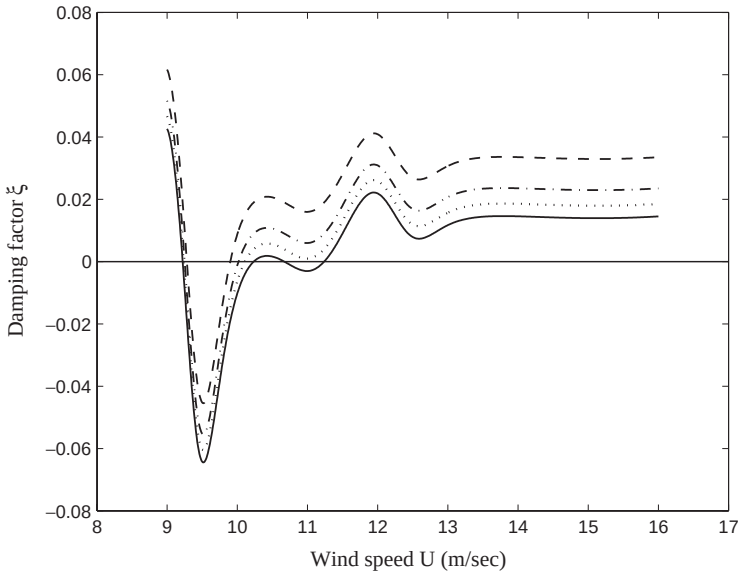

Fig. 4. Damping factor ξ versus wind speed U: ⋯, $\xi_0 = 0.001$; – –, $\xi_0 = 0.005$; –·–, $\xi_0 = 0.010$; —, $\xi_0 = 0.020$.

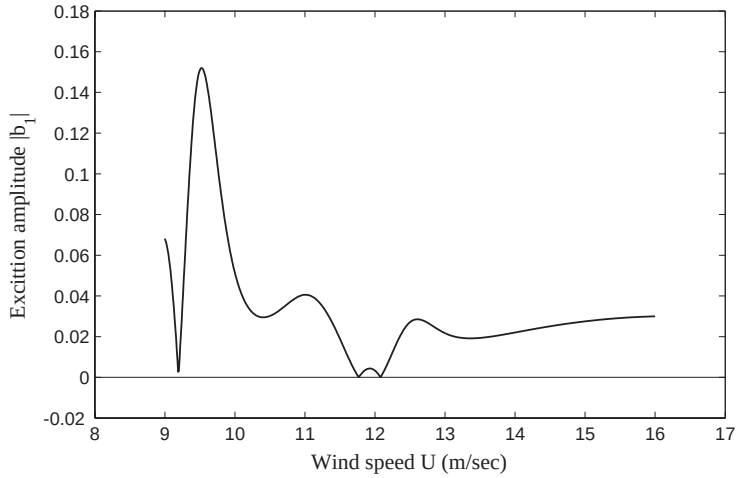

Fig. 5. The amplitude of b_1 versus wind speed.

The damping factor ξ_f of the filter, which may be estimated from wind–rain tunnel tests or field measurements, is chosen as $\xi_f = 0.02$. A typical PSD in the frequency range $0 \leqslant \omega \leqslant 3$ of the output of the narrowband filter (13) for $\omega_f = 1.2$ is shown in Fig. 6, where σ_ϕ^2 given by Eq. (19) depends on the constants ω_f, ξ_f and S_0. Based on the measured data from the wind tunnel test, as shown in Figure 13 of Ref. [1] for the variation of upper rivulet circumferential oscillation with wind speed, the amplitude of the rivulet motion $\phi(t)$ is about $\pi/18$. Thus, the value of σ_ϕ is about $\pi/(18\sqrt{2})$.

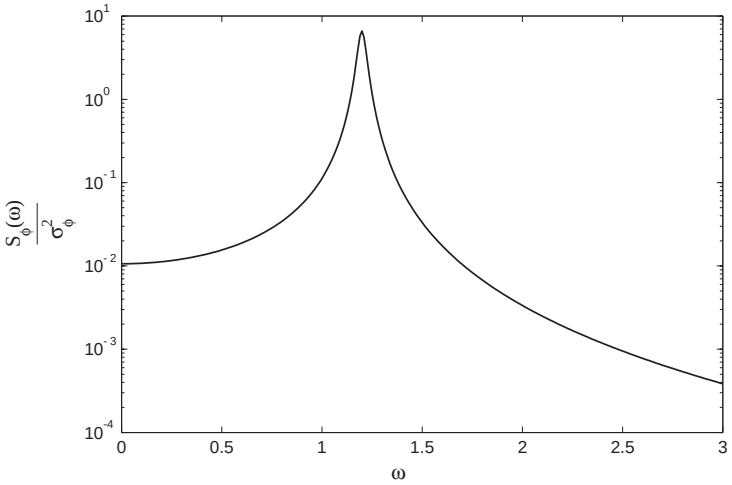

Fig. 6. PSD of the fluctuation angle $\phi(t)$ for $\omega_f = 1.2$.

As mentioned before, when the damping factor ξ is negative, instead of the linearized model, a non-linear model should be investigated in the analysis of dynamic response. When the damping factor ξ is positive, the response process of the linear system will be stationary (once transients have decayed away); thus, the stochastic response derived in the last section can be used to evaluate the response amplitude of the stay cables in wind–rain conditions. The structural damping ratio is now set to $\xi_0 = 0.006$ such that the damping factor ξ is positive for mean wind speeds of 9, 11, 13 and 15 m/s, respectively.

Fig. 7 shows the PSD in the frequency range $0 \leqslant \omega \leqslant 3$ of the response $\bar{y}(t)$ for mean wind speeds of 9, 11, 13 and 15 m/s, respectively. It is seen that the height of the spectral peak depends on the mean wind speed.

Fig. 8 shows the standard deviation of the stochastic response $y(t)$ against the filter frequency for mean wind speed of 9, 11, 13 and 15 m/s, respectively. Obviously, the peak response depends on the filter frequency. According to the wind tunnel test observation [1], the rivulet oscillates in a circumferential direction with the same period of the cable motion. Thus, the filter frequency is $\omega_f \approx 1$ with respect to the dimensionless t.

As indicated in the last section, the absolute value of $C_l'(\alpha)$ is expected to be rather small due to the small size of the rivulet relative to D. In this situation, the damping factor ξ is positive because $C_l'(\alpha) + C_d(\alpha)$ is positive. In the present example, however, since the diameter ratio of rivulet to cable is 0.1 which is much larger than the actual diameter ratio, the absolute value of $C_l'(\alpha)$ is not small. So, in order to investigate the stochastic response $y(t)$ against the mean wind speed, the structural damping ratio is set to $\xi_0 = 0.08$ such that the damping factor ξ is positive for mean wind speed range from 9 to 16 m/s, in spite of the actual structural damping ratio being quite small.

Fig. 9 shows the standard deviation of the stochastic response $y(t)$ against the mean wind speed for filter frequency of 0.9, 1.0, 1.2 and 1.5, respectively. It can be seen that, at a wind speed of about 9.2 m/s, the standard deviation increases with the increasing wind speed until the peak

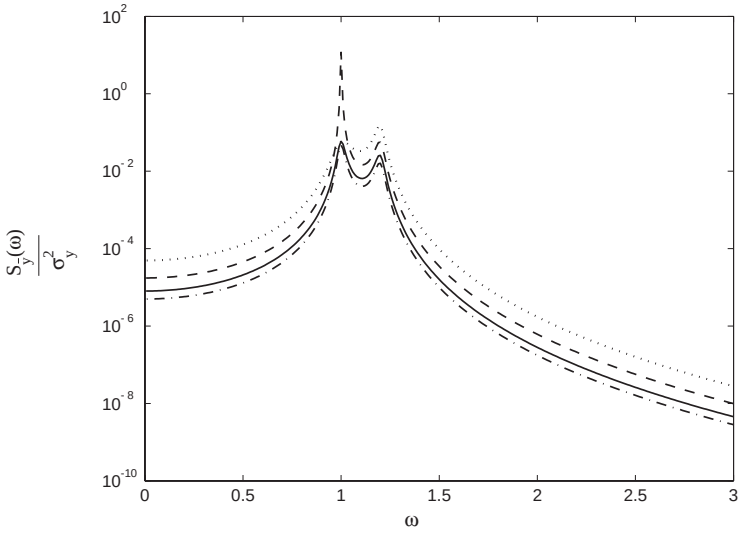

Fig. 7. PSD of the response for $\omega_f = 1.2$: ⋯, $U = 9$ m/s; – –, $U = 11$ m/s; –·–, $U = 13$ m/s; —, $U = 15$ m/s.

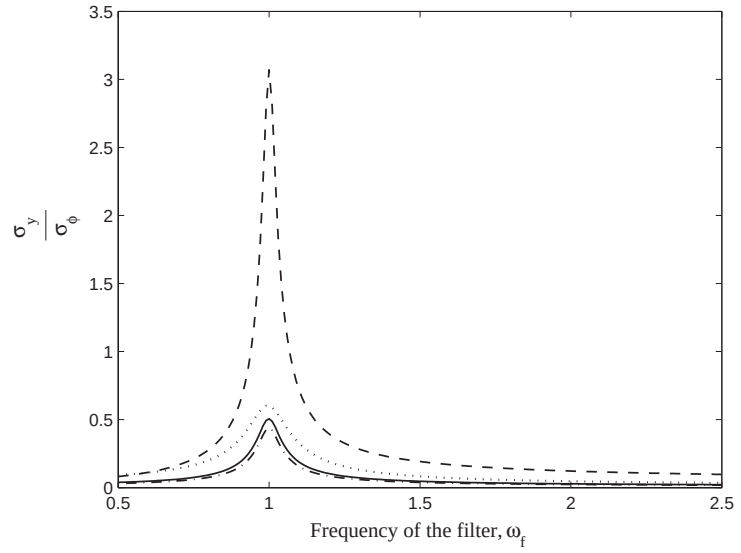

Fig. 8. Standard deviation of response versus filter frequency: ⋯, $U = 9$ m/s; – –, $U = 11$ m/s; –·–, $U = 13$ m/s; —, $U = 15$ m/s.

response is reached. After the peak response, the standard deviation decreases to a lower level with a further increase of wind speed. The peak response depends on the filter frequency. The peak response is quite small if the filter frequency is far from the natural frequency of the cable.

Based on the measured static rivulet positions on cylinders and drag and lift coefficients from wind tunnel tests, the above results are qualitatively compatible with the observations of wind–rain-induced cable vibrations from field measurements. On the other hand, since $\sigma_Y = U\sigma_y/\omega_n$,

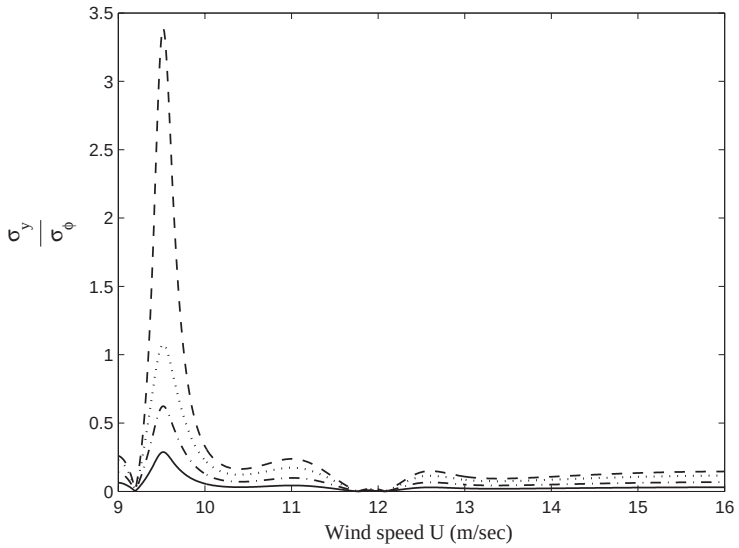

Fig. 9. Standard deviation of response versus wind speed: ⋯, $\omega_f = 0.9$; – – $\omega_f = 1.0$; –·–, $\omega_f = 1.2$; —, $\omega_f = 1.5$.

the peak standard deviation can be estimated for $\xi_0 = 0.08$, $\xi_f = 0.02$, $\omega_f = 1.0$ and $\sigma_\phi = \pi/(18\sqrt{2})$ as

$$\sigma_Y = \frac{U\sigma_y}{\omega_n} = \frac{9.52}{2.12} \times 3.3899 \times \frac{\pi}{18\sqrt{2}} = 1.8787 \quad \text{(m)}.$$

Thus, the response amplitudes of the cylinder predicted here are somewhat larger than some measured data, even when the structural damping ratio is taken to be as large as 0.08. This is probably due to our use of drag and lift coefficients obtained from tests on structures with rivulets whose size is large compared to the diameter of the cable. Thus, further wind tunnel investigations of the vibrations of cables with artificial rivulets would be beneficial to the analysis.

5. Conclusions

A stochastic model describing the vertical motion of a spring-mounted model of a cross-section of a stay cable with a mobile rivulet (produced by the combined effect of wind and rain) has been constructed. The stochastic response of the model with linearized aerodynamic forces has been analyzed.

Using experimentally measured static rivulet positions on cylinders and drag and lift coefficients from wind tunnel tests the dynamics of a single cable has been explored in this stochastic model. The PSD and standard deviation of certain responses have been calculated. By varying parameters in the model it is apparent that a stochastic resonant phenomenon can be induced that depends stochastically on the location of the rivulet. Due to this motion, the cable experiences stochastic excitation. For appropriate parameters, the system can rapidly evolve to a stationary stochastic state. In general, the steady stochastic response amplitude depends on C_l and C_d, the structural damping ratio ξ_0, as well as the parameters w_f, ξ_f and S_0. The dependence of the

response on these parameters has been explored. Unlike the Den Hartog mechanism (in which galloping is related to an instability due to effective anti-damping) this model predicts stochastic resonance with effective positive damping throughout.

In many practical situations, the absolute value of $C_l'(\alpha)$ is expected to be rather small for a small-size rivulet relative to the diameter of the cable. This leads to positive aerodynamic damping. In such cases, the above analysis suggests a mechanism for large amplitude vibrations of stay cables due to stochastic excitations by moving rivulets. If the structural damping is such that this leads to wind–rain-induced galloping, $\xi \leqslant 0$, the dynamic behaviour of the cable could depend on neglected terms in the expansion of the aerodynamic force and is therefore outside the scope of the linearized model discussed here. Such non-linear behaviour will be discussed elsewhere.

Acknowledgements

The authors are most grateful to S.W. Smith (U. Kentucky, USA) for stimulating interactions and to the EPSRC and Royal Academy of Engineering for financial support in this study.

References

[1] Y. Hikami, N. Shiraishi, Rain–wind induced vibration of cables in cable stayed bridges, Journal of Wind Engineering and Industrial Aerodynamics 29 (1988) 409–418.
[2] R.W. Poston, Cable-stay conundrum, Civil Engineering 68 (1998) 58–61.
[3] J.H.G. Macdonald, E.L. Dagless, B.T. Thomas, C.A. Taylor, Dynamic measurements of the Second Severn Crossing, Proceedings of the Institution of Civil Engineers, Transport 123 (1997) 241–248.
[4] J.L. Lilien, A. Pinto da Costa, Vibration amplitudes caused by parametric excitation of cable stayed structures, Journal of Sound and Vibration 174 (1994) 69–90.
[5] A. Pinto da Costa, J.A.C. Martins, F. Branco, J.L. Lilien, Oscillations of bridge stay cables induced by periodic motions of deck and/or towers, Journal of Engineering Mechanics, American Society of Civil Engineers 122 (1996) 613–622.
[6] P. Warnitchai, Y. Fujino, T. Susumpow, A non-linear dynamic model for cables and its application to a cable-structure system, Journal of Sound and Vibration 187 (1995) 695–712.
[7] H. Yamaguchi, Analytical study on growth mechanism of rain vibration of cables, Journal of Wind Engineering and Industrial Aerodynamics 33 (1990) 73–80.
[8] M. Matsumoto, T. Saitoh, M. Kitazawa, H. Shirato, T. Nishizaki, Response characteristics of rain–wind induced vibration of stay-cables of cable-stayed bridges, Journal of Wind Engineering and Industrial Aerodynamics 57 (1995) 323–333.
[9] A. Bosdogianni, D. Olivari, Wind- and rain-induced oscillations of cables of stayed bridges, Journal of Wind Engineering and Industrial Aerodynamics 64 (1996) 171–185.
[10] C. Versiebe, Exciting mechanisms of rain–wind-induced vibrations, Structural Engineering International 8 (1998) 112–117.
[11] J.P. Den Hartog, Transmission line vibration due to sleet, AIEE Transactions 51 (1932) 1074–1076.
[12] R.D. Blevins, W.D. Iwan, The galloping response of a two-degree-of-freedom system, Transactions of the American Society of Mechanical Engineers, Journal of Applied Mechanics 41 (1974) 1113–1118.
[13] P. Yu, A.H. Shah, N. Popplewell, Inertially coupled galloping of iced conductors, Transactions of the American Society of Mechanical Engineers, Journal of Applied Mechanics 59 (1992) 140–145.
[14] K.F. Jones, Coupled vertical and horizontal galloping, Journal of Engineering Mechanics, American Society of Civil Engineers 118 (1992) 92–107.

[15] A. Luongo, G. Piccardo, Non-linear galloping of sagged cables in 1:2 internal resonance, Journal of Sound and Vibration 214 (1998) 915–940.
[16] P. Yu, Y.M. Desai, A.H. Shah, N. Popplewell, Three-degree-of-freedom model for galloping, part I: formulation, Journal of Engineering Mechanics, American Society of Civil Engineers 119 (1993) 2404–2425.
[17] P. Yu, Y.M. Desai, N. Popplewell, A.H. Shah, Three-degree-of-freedom model for galloping, part II: solutions, Journal of Engineering Mechanics, American Society of Civil Engineers 119 (1993) 2426–2448.
[18] D.Q. Cao, R.W. Tucker, C. Wang, Aeroelastic stability of a Cosserat stay cable, Proceedings of the Fourth International Symposium on Cable Dynamics, Montreal, Canada, 2001, pp. 369–376.
[19] M. Falco, F. Fossati, F. Resta, On the vortex-induced vibration on submarine cables: design optimization of wrapped cables for controlling vibrations, Proceedings of the Third International Symposium on Cable Dynamics, Trondheim, Norway, 1999.
[20] D.Q. Cao, R.W. Tucker, C. Wang, Stability analysis of stay cables with moving rivulets, Lancaster University, preprint, 2002.